

The 10th International Congress of The International Radiation Protection Association
14-19 May 2000, Hiroshima, Japan

Retrospective Dosimetry

Peter Jacob
GSF - National Research Center for Environment and Health
Institute of Radiation Protection
D-85764, Neuherberg, Germany

Three methods of *Retrospective Assessment of Exposures to Ionizing Radiation* are reviewed:

First, electron paramagnetic resonance (EPR or ESR) with teeth has its strengths in the determination of individual external exposures or homogeneous internal exposures that may have occurred several decades ago. The method is best suited for photon fields. The current detection limit is 100 mGy. Due to a higher sensitivity to photons with energies in the range of 30 to 100 keV, information of this spectral component is necessary to achieve a high accuracy. The method itself is capable to give indications about this contribution by separate analyses of inner and outer parts of the teeth.

Second, luminescence methods including thermoluminescence (TL) and optical stimulated luminescence (OSL) have their strengths in determining absorbed dose in bricks or porcelain. Detection limits depend on the amount of dose due to natural radiation field and are in the order of several tens of mGy. By measuring depth profiles of absorbed dose in a brick or height profiles over a wall, information on source geometry and photon energy may be obtained.

Third, modelling based on environmental measurements has its strengths in the assessment of dose of larger population groups. Expertise on time dependencies that was gained after past radionuclide releases to the environment can be used in the form of analytical approximations. Validation by measurements of radionuclide contents in the human body or of individual external exposures by TLD's improve confidence in the results.

Case studies in which different methods are applied to the same individuals or areas are used for comparative analyses.

Future perspectives of the methods include: Conversion of dose quantities measured as absorbed dose in dentine or bricks to absorbed dose in human organs; *in situ* EPR measurements of teeth in the human mouth; and exploration of new materials for the luminescence method, especially those which are worn by people allowing to come closer to an individual dosimetry.

Method	Type of exposure			
	External	Internal, α	Internal, β	Internal, γ
EPR		-		
Luminescence		-	-	-
Chromosome aberrations		-	-	
Radionuclides in human body	-			
Radionuclides in environment				

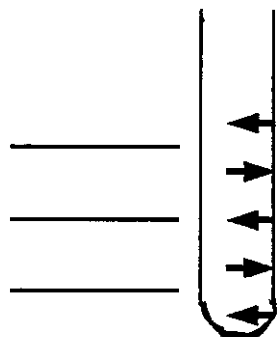
Individual dose

Individuel dose
Individual dose

Group dose

Methods of the upper panel are related to dose, methods of the lower panel to dose rate.

X-Band EPR Dose Reconstruction with Enamel Powder



$$\Delta E_H = H \cdot g \cdot \beta$$

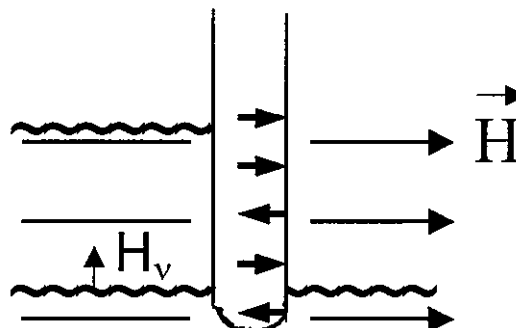
Magnetic field $H = 0.35 \text{ T}$

Landé factor $g \sim 2.002$

Bohr magneton

$\beta = 9.3 \cdot 10^{-24} \text{ J/T}$

about 50.08% of
magnetic moments
are antiparallel to H



$$E_{\text{mw}} = h \cdot v$$

Planck constant

$h = 6.6 \cdot 10^{-34} \text{ J} \cdot \text{s}$

Microwave frequency

$v = 9.8 \cdot 10^9 \text{ Hz}$

maximally 50% of
magnetic moments
can be parallel to H

$$\Delta E_H = E_{\text{mw}} = 6.5 \cdot 10^{-24} \text{ J}$$

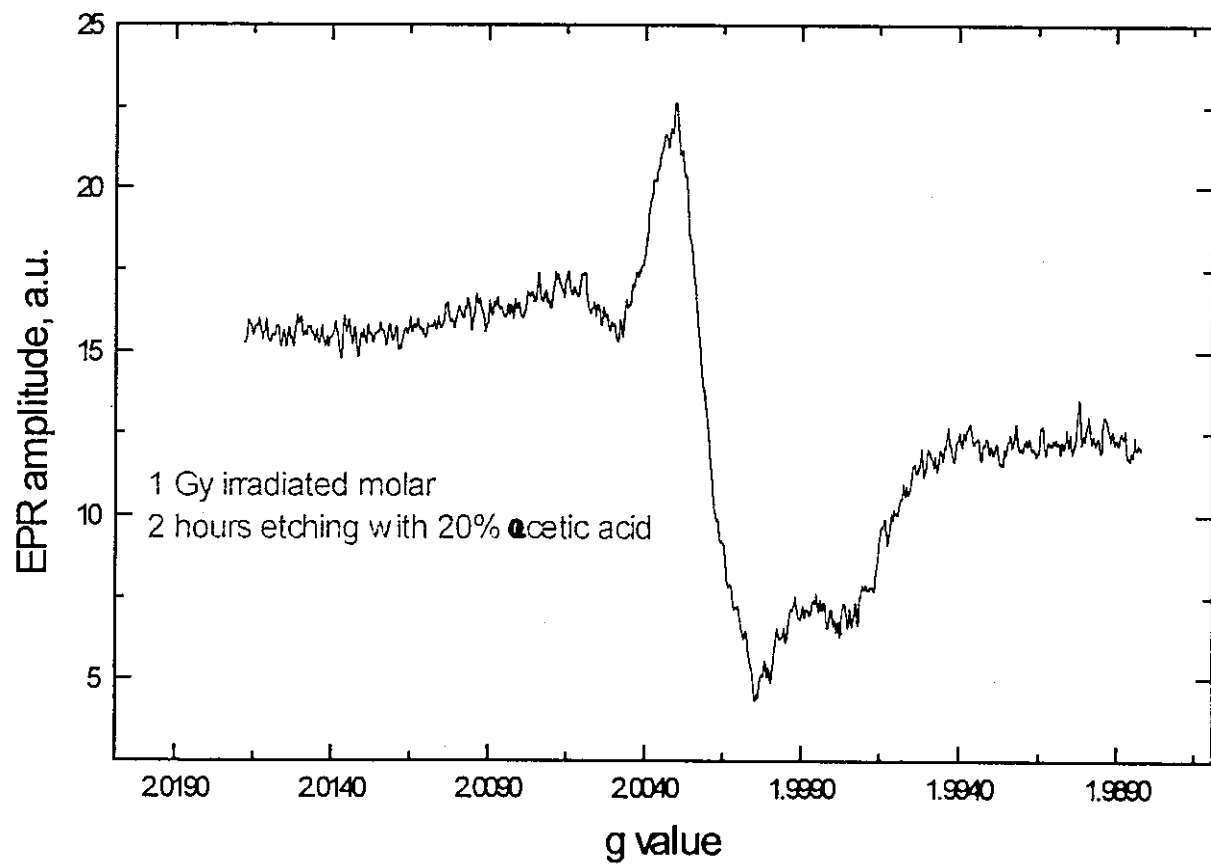
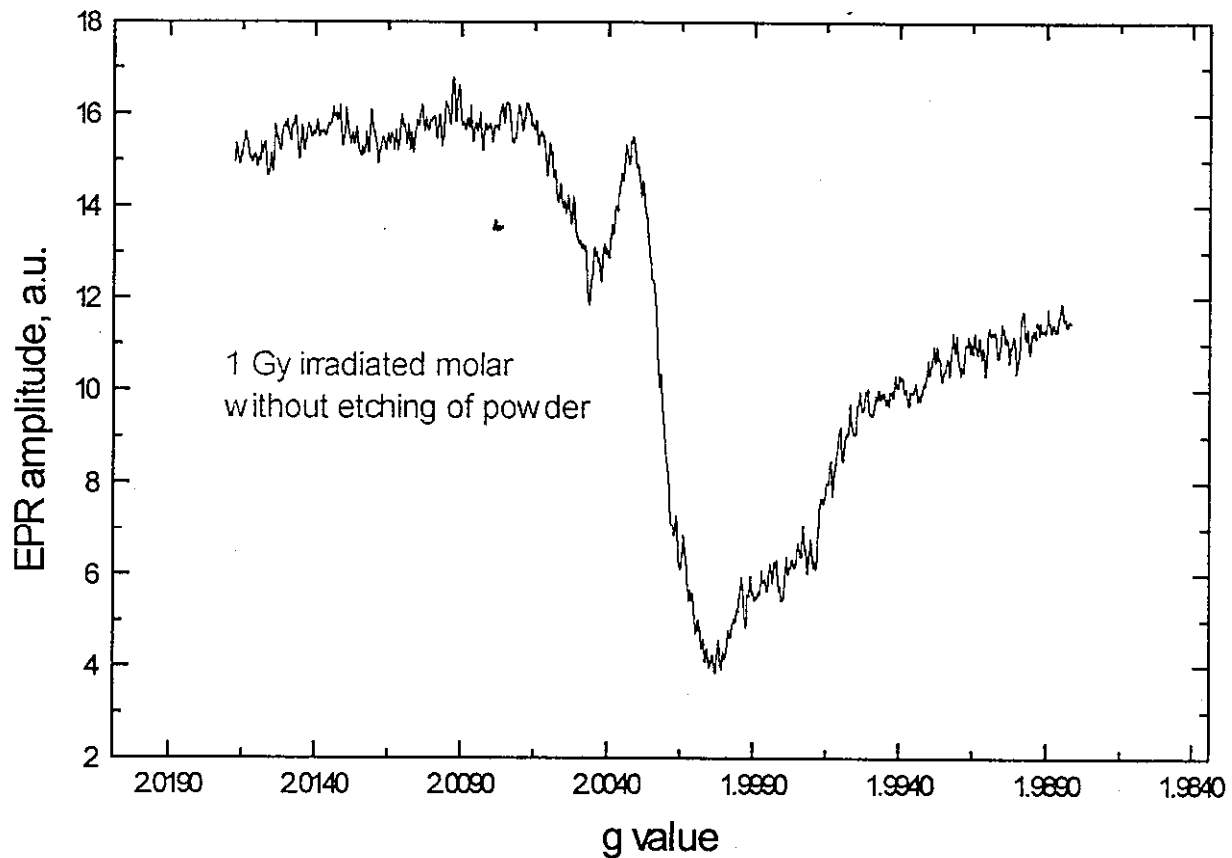
EPR with teeth

Three sample preparation techniques:

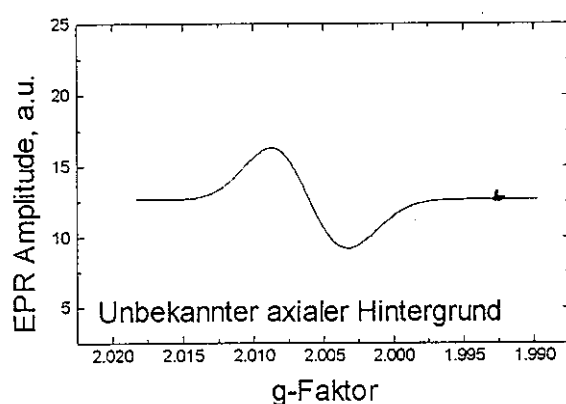
- a) Mechanical method: Dentine removed by drill, enamel ground to grain size 0.5-1 mm. No etching.
- b) Semi chemical method: Dentine removed by drill, controlled by fluorescence of 360nm UV-light. Enamel ground to grain size 0.5-2 mm and etched with orthophosphoric acid.
- c) Chemical method: Dentine removed by sodium hydroxide solution in an ultra sonic cleaner. Enamel ground to grain size 0.1-0.6 mm and etched with acetic acid.



Grinding effects

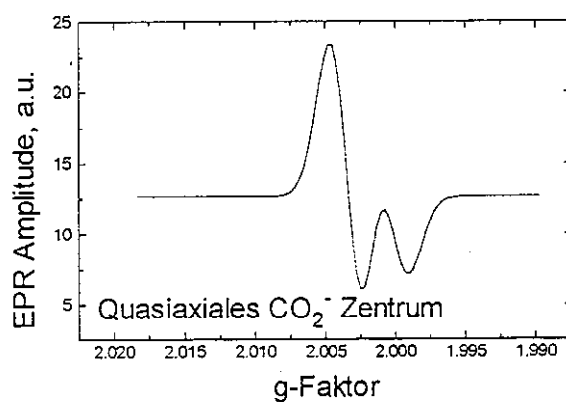


Gaußsche Komponenten der EPR Simulation



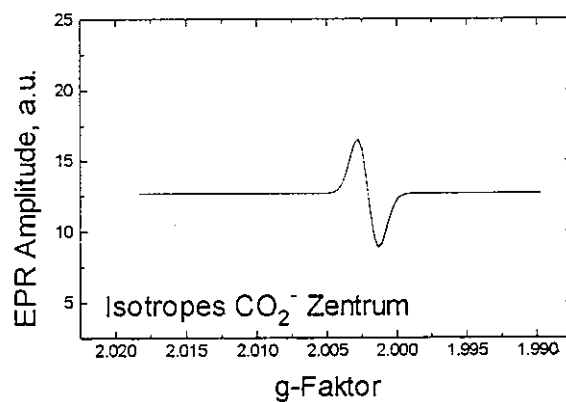
Parameter:
(expositionsunabhängig)

$g_{\perp} = 2.0052$
 $g_{\parallel} = 2.0026$
 $\Delta H_{pp} = 0.80 \text{ mT}$

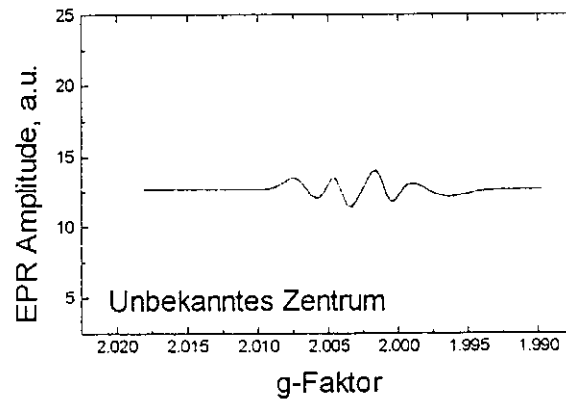


(expositionsabhängig)

$g_{\perp} = 2.0019$
 $g_{\parallel} = 1.9993$
 $\Delta H_{pp} = 0.54 \text{ mT}$

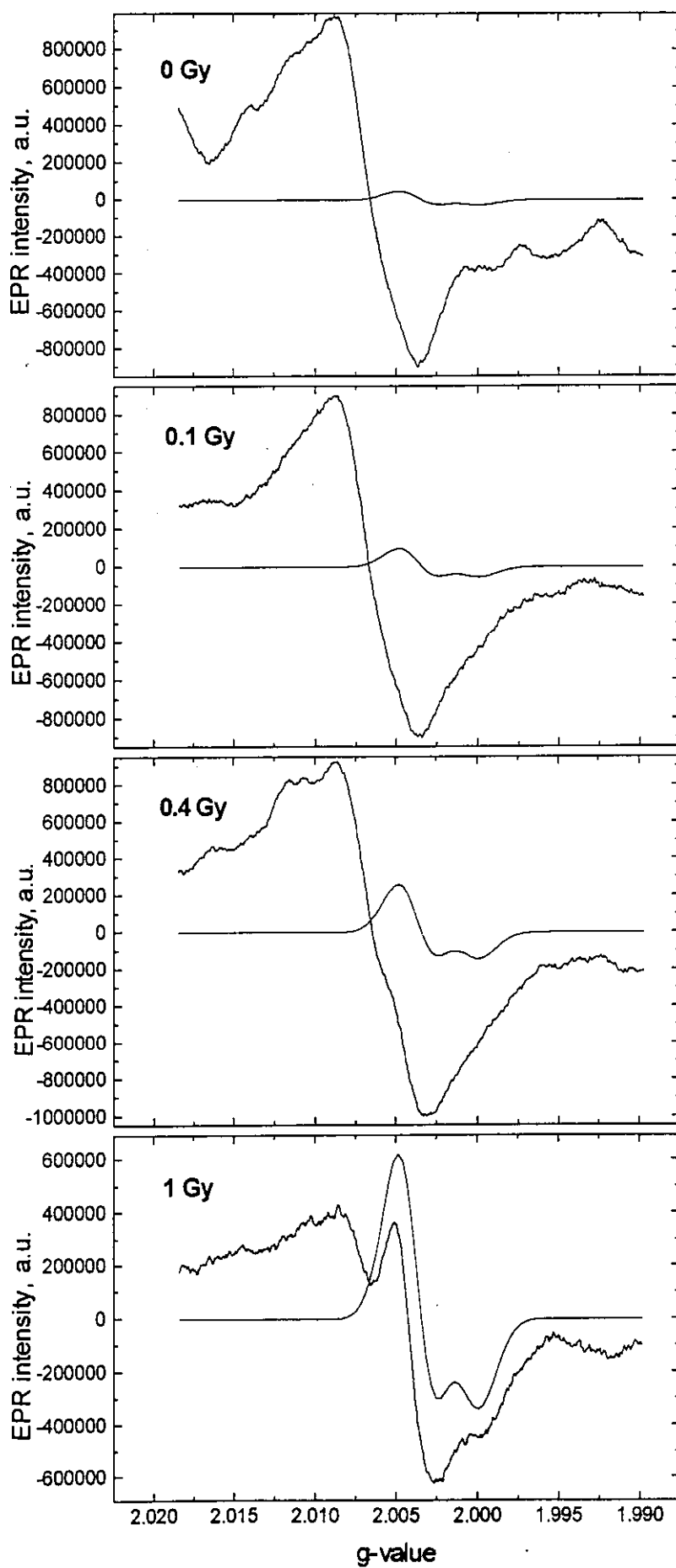


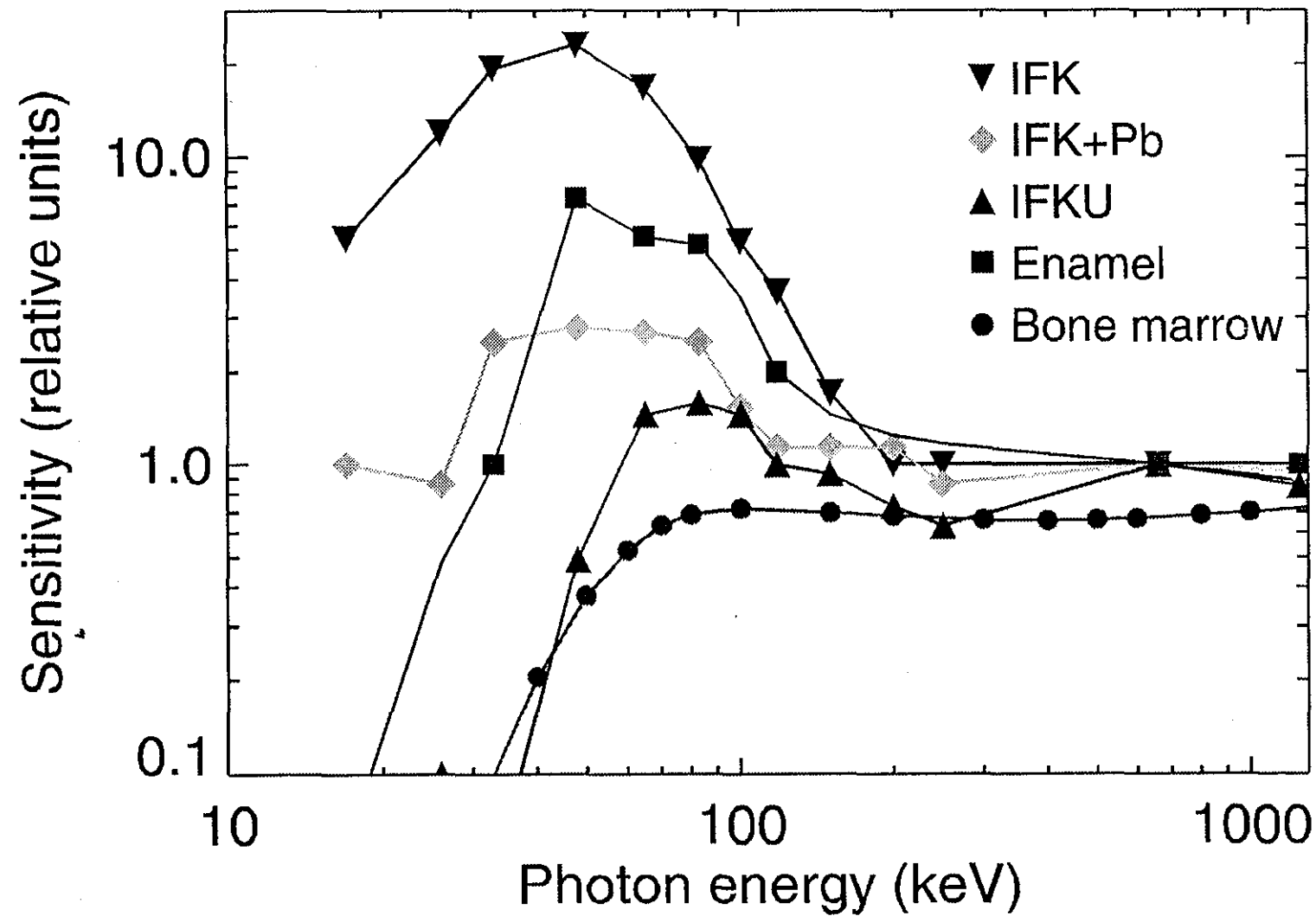
$g = 2.0006$
 $\Delta H_{pp} = 0.30 \text{ mT}$



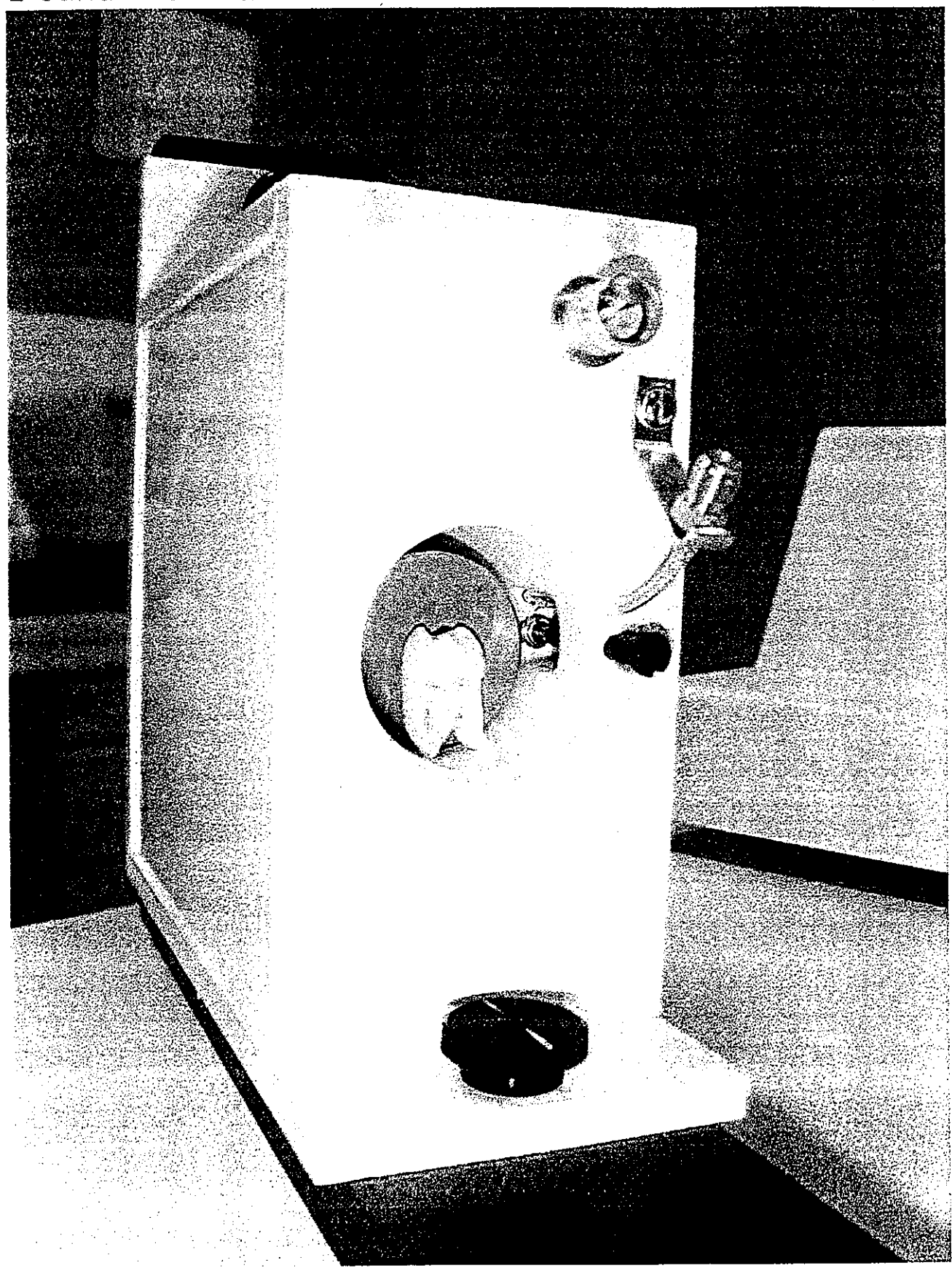
$g_1 = 2.0050$
 $g_2 = 2.0026$
 $g_3 = 1.9995$
 $g_4 = 1.9967$
 $\Delta H_{pp} = 0.27 \text{ mT}$

EPR spectra of tooth enamel and content of CO_2^- radicals



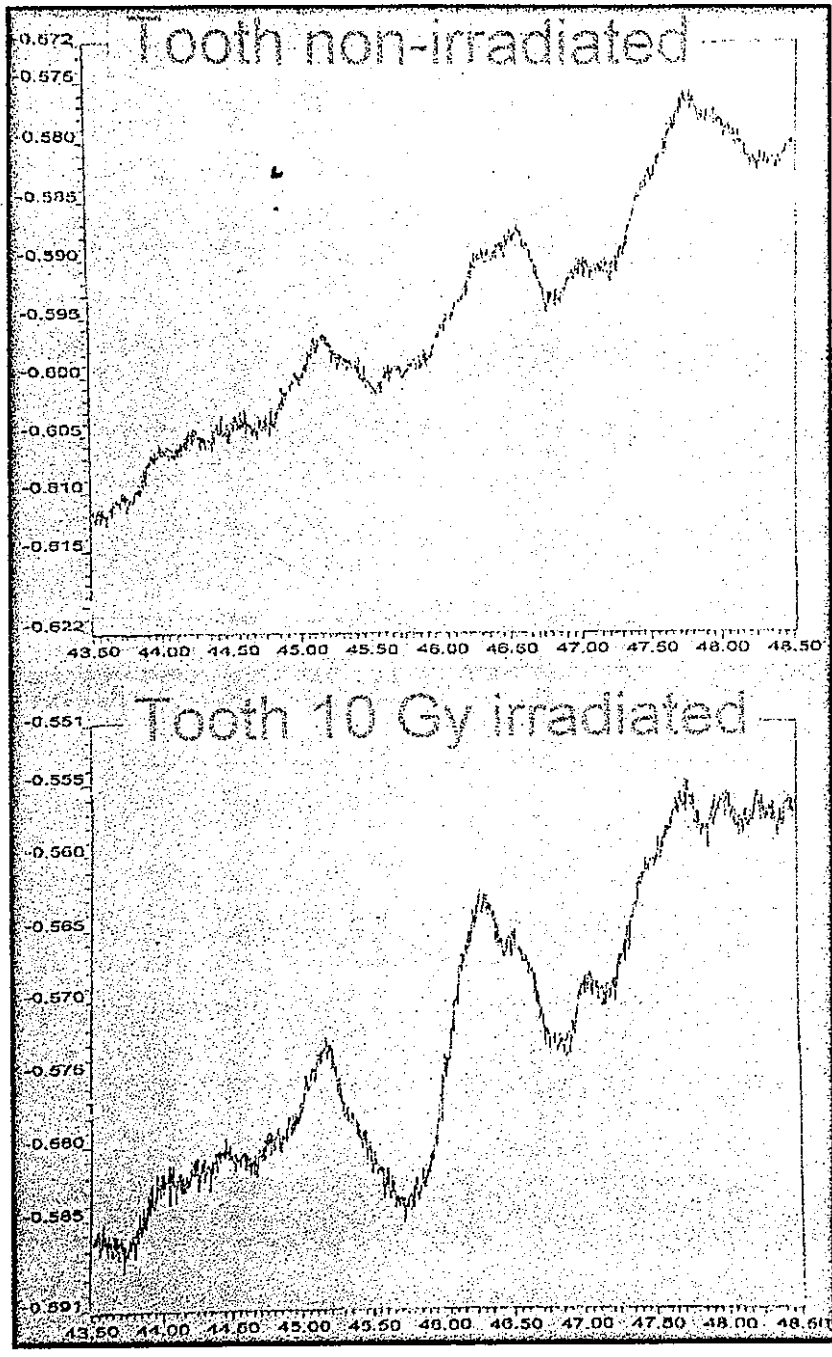


L-band microwave cavity



L-band EPR spectra

Relative EPR intensity



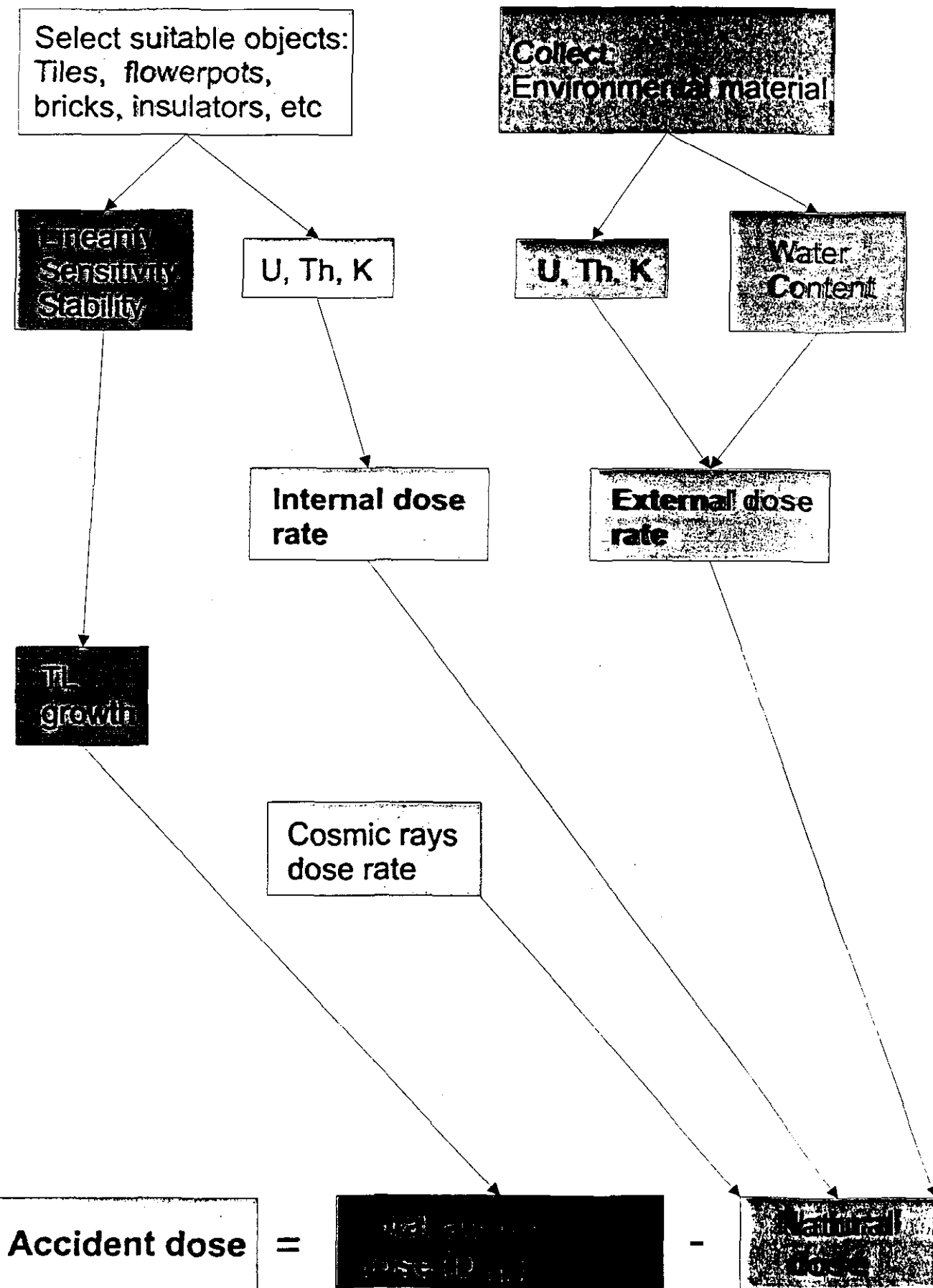
EPR spectra provided by:
Rene Debuyst, UCL, Brussels, Belgium

X- and L-band in comparison

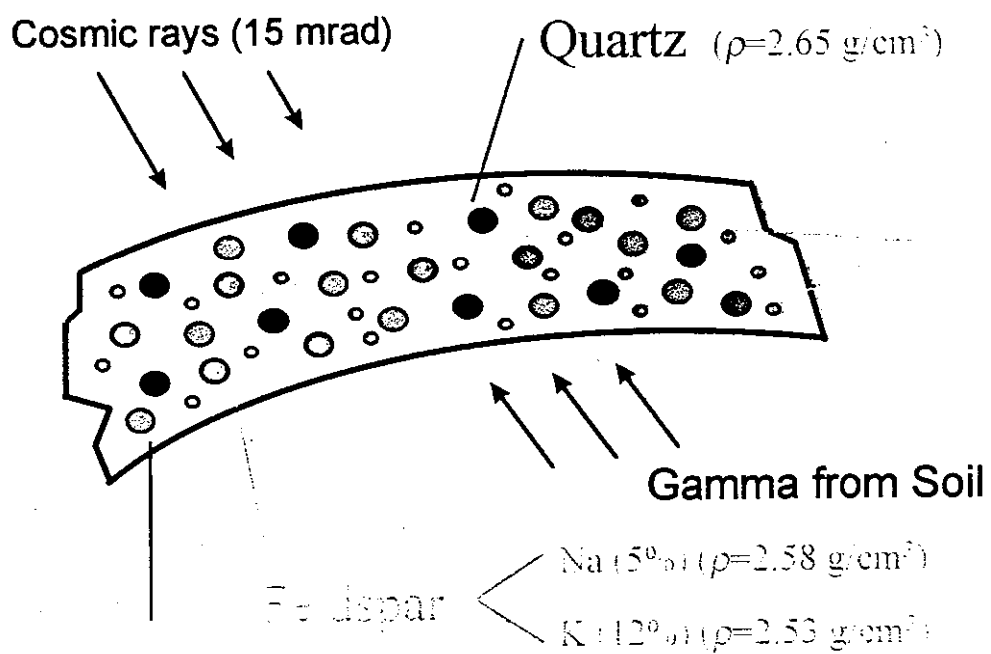
	X-band	L-band
Microwave freq., GHz	9.8	1.3
Magnetic field at g=2, mT	350	46
Max. sample volume, cm ³	8	3400
Rel. dielectric losses by water	1	0.2
Rel. sensitivity for unlimited samples with dielectric losses	1	2
Rel. resolution of g-value differences	1	0.1
Lower appl. range in EPR tooth dosimetry, mGy	100	200 [#]

[#] expected by Miyake et al. (2000), *Appl.Radiat.Isot* **52**, 1031-1038

LUMINISCENCE METHODS OF ACCIDENT DOSE ASSESSMENT



Luminescence in Bricks



Heavy minerals like
zircon apatite etc.

$\rho = 2.65 \text{ g/cm}^3$

- Magnetic separation
- Heavy liquid separation

Natural Radioactivity Contents

Th: 12-20 ppm
U : 3-10 ppm
K : ~ 1 %

Methods Available

- * Fine grain
- * Pre-dose
- * Quartz incl.
- * Feldsp. incl.
- * Zircon incl.
- * Subtraction
- * OSL green (Quartz)
- * OSL IR (Feldspar)

Dose Rate (mGy/year for 1 ppm)

	α	β	γ
Th-series	0.73	0.03	0.05
U- series	2.78	0.14	0.11
K (1 %)	-	0.68	0.20

Standard geological techniques to

Extract required mineral fraction

from ceramic materials.

e.g. quartz of grain size 50-150 μm

is obtained by crushing, sieving
and heavy liquid separation

aliquots $\sim 2 \text{ mg}$) can be extracted

from 10-20 g of brick.

grains are etched in HF to
remove material in which particles

work under dim red light.

$\approx 17^{\text{BG}} \sim 2-4 \text{ mg} \cdot \text{y}^{-1}$

were absorbed

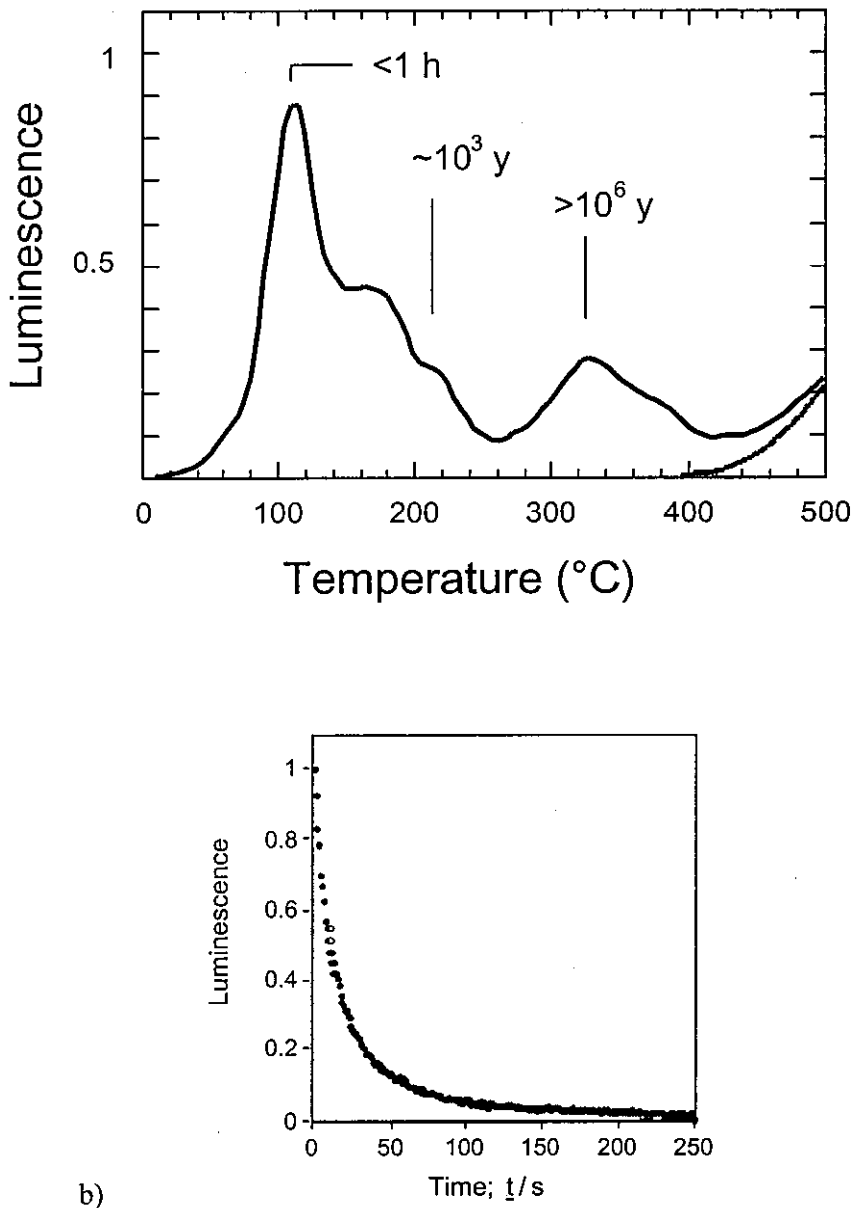
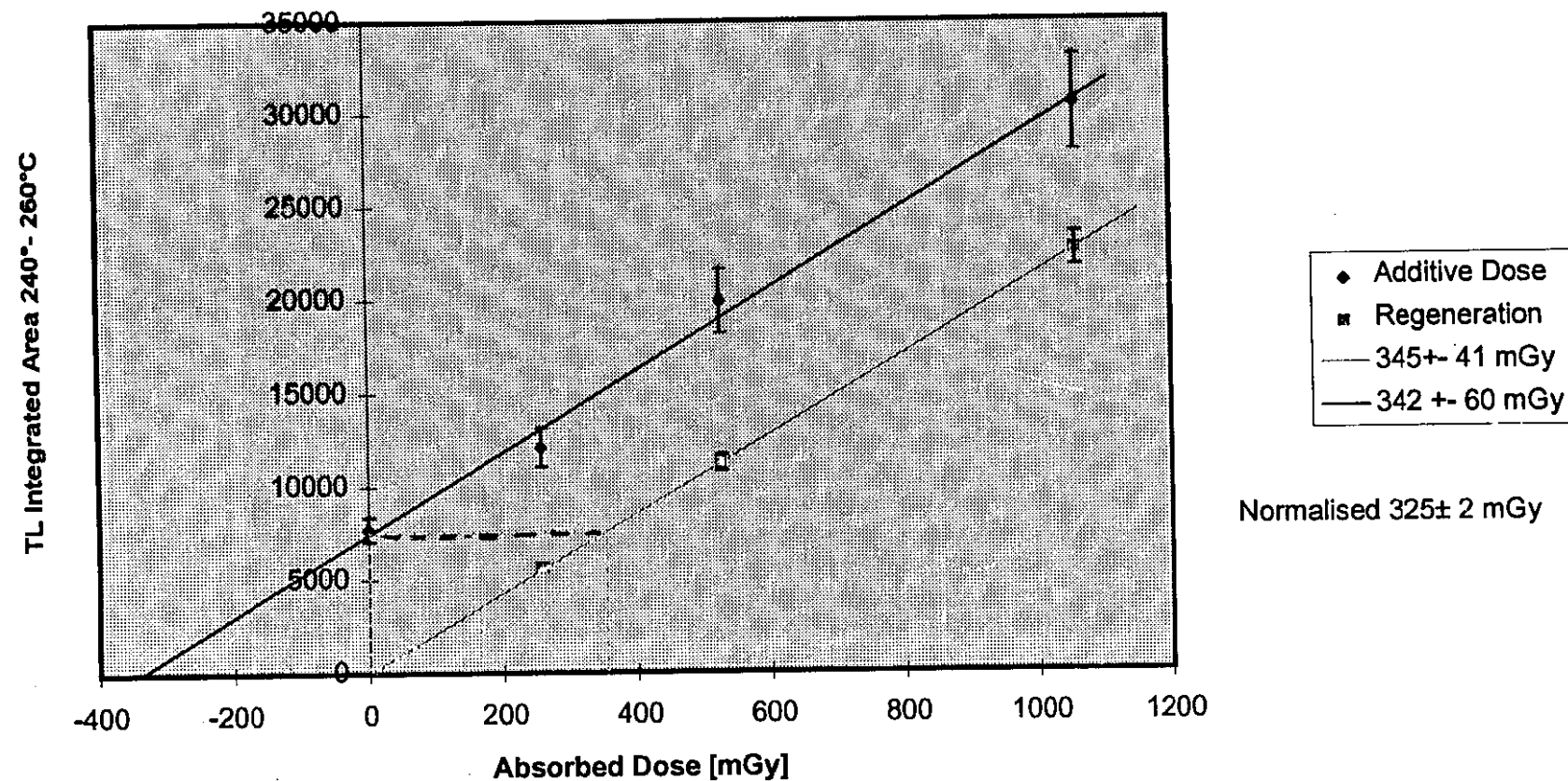
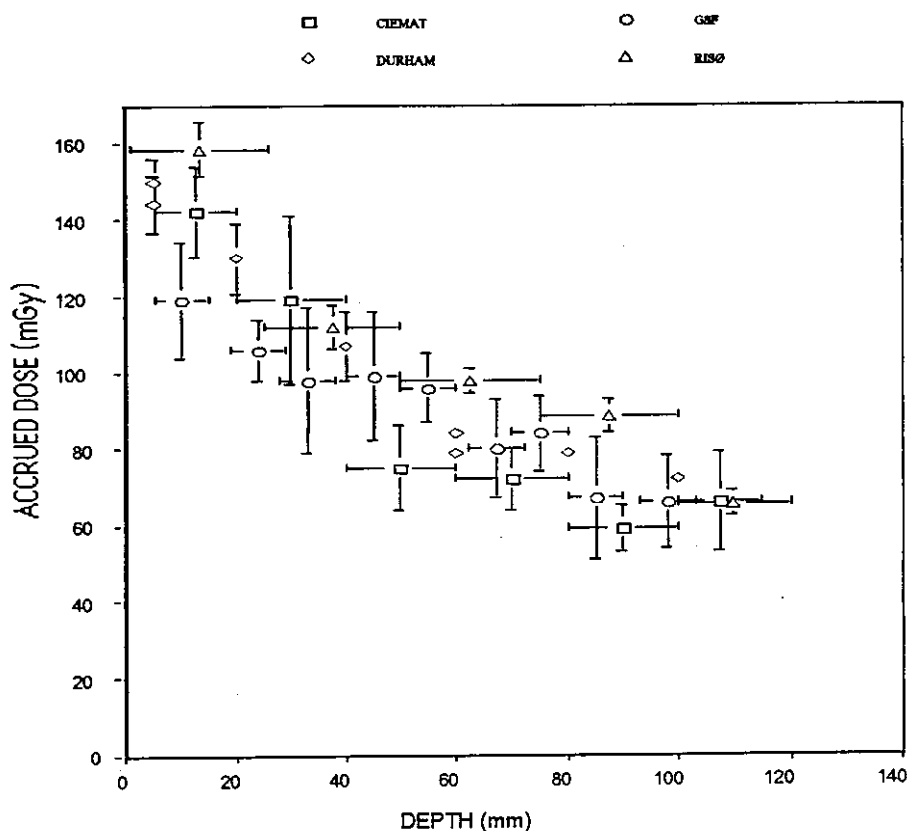


Figure 4.1.1 Examples of luminescence signals recorded with quartz samples: a) a TL glow curve recorded as a function of temperature, T , measured while heating a sample at a constant rate of 5 $^{\circ}\text{C}/\text{s}$. The mean lifetimes at room temperature are indicated for traps associated with TL peaks located at ~ 110 , ~ 210 and ~ 325 $^{\circ}\text{C}$, and b) OSL intensity vs time, t , measured while stimulating the sample with visible light (470-540 nm) at constant intensity and maintaining the sample at constant temperature (75 $^{\circ}\text{C}$).

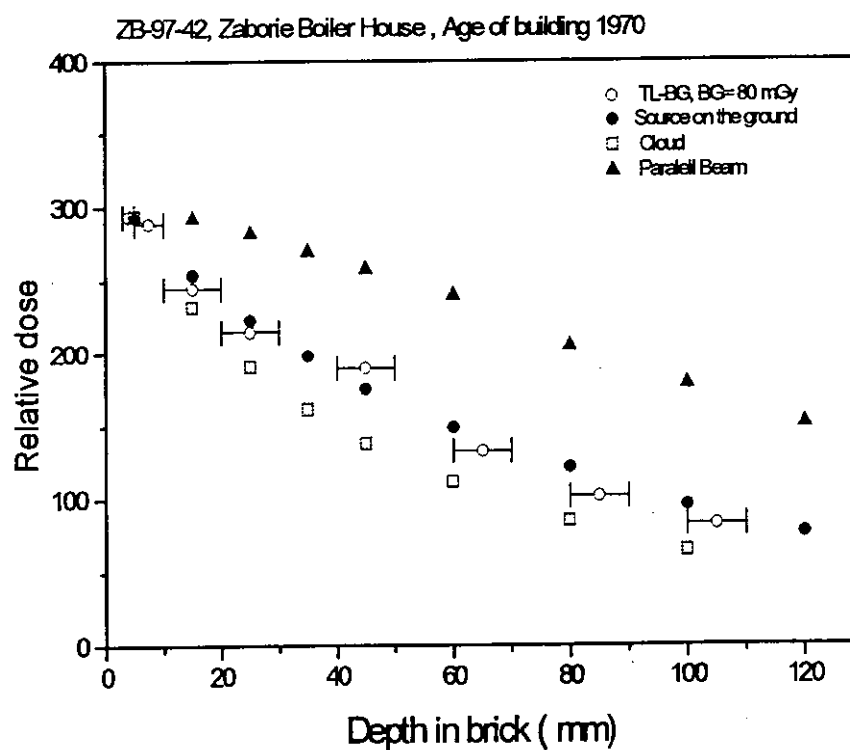
Zaborie 97 location No.: 42 d=1.5 cm



NOVOZYBKOV NZ95-1



Results of different luminescence methods for absorbed dose in a brick.



Comparison of measured depth dose profile with Monte Carlo calculations for different source geometries.

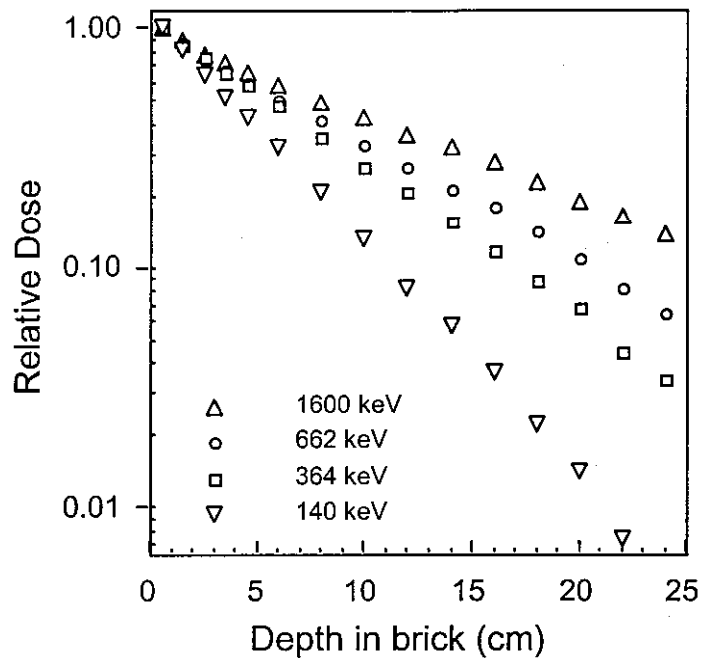


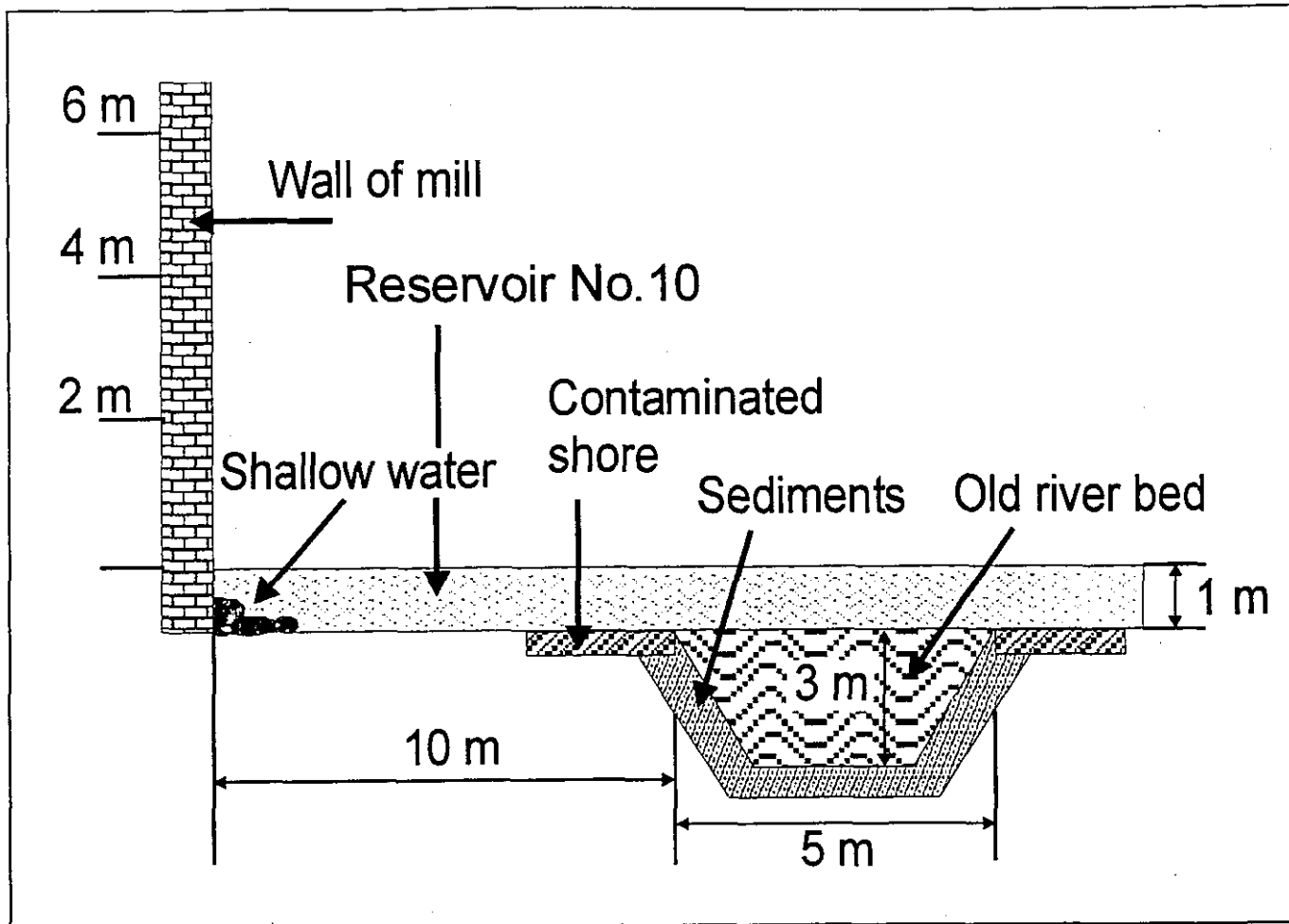
Figure 4.1.5a. Calculated depth dose profiles at an height of 1 m above ground level in a brick wall exposed to gamma radiation originating from radionuclides deposited on the ground, for source energies of 140 keV, 364 keV, 662. keV and 1600 keV. The depth dose distributions have been normalized to the respective dose in the first depth layer of the brick wall.

2 Table 6.3 - Ratio of dose in brick at sampling locations of different heights above ground level to the dose in
 3 brick at a height of 1 m for gamma radiation from a semi - infinite radioactive cloud (A) and from radionuclides
 4 distributed on the ground surface within various distances from the wall and also within a layer : to a distance
 5 of 200m on the surface (B) and within a layer of thickness 5 g cm^{-2} (C), deposited on the ground to a distance of
 6 35 m (D) and between 35 m and 100 m (E). The source energy is 662 keV.

7

Height m	Radionuclide distribution				
	(A) Semi-infinite cloud	(B) ground surface 0 - 200 m	(C) 5 g cm^{-2} layer 0 - 200 m	(D) ground surface 0 - 35 m	(E) ground surface 35 - 100 m
1	1.00	1.00	1.00	1.00	1.00
4	1.11	0.73	0.90	0.64	1.04
10	1.19	0.56	0.83	0.40	1.10
18	1.23	0.44	0.68	0.26	1.15

8



Ratio of doses in brick

Simulations

Height of sampling (m)	Simulations					
	Measured	River sediments	Shore of river	Reservoir close to wall	Shore of reservoir	Rest of reservoir
6	0.5	1.8	1:3	0.2	0.8	1.1
4	0.7	1.4	1.2	0.4	0.9	1.0
2	1.0	1.0	1.0	1.0	1.0	1.0

Ratio of absorbed dose in brick (at a height of 1m above ground and at a depth of 5-15 mm in the wall) to air Kerma above an open field.

Source geometry	Photon energy (keV)		
Ground	140	364	662
Cloud	1600		
	0.86	0.57	0.51
	0.72	0.55	0.52
			0.48

Ratio of absorbed dose in brick (at a height of 1m above ground and at a depth of 5-15 mm in the wall) to air Kerma above an open field. Source energy is 662 keV and the contaminated wall is assumed to have an activity per unit area of 10% of the open field.

	Homogeneous source Surface	Heterogeneous source ($0.1 \text{ g} \cdot \text{cm}^{-2}$)
Wall	$0.30 \text{ g} \cdot \text{cm}^{-2}$	$A_{0-2\text{m}} = 2 * A$
Uncontaminated	0.51	0.54
Contaminated	0.56	0.83
	0.68	0.32
	0.76	0.39

$A_{0-4.5\text{m}} = 0.2 * A$

Example of Modelling Based on Environmental Measurements:

Reconstruction of radiation exposures of evacuees from the 30-km zone around the Chernobyl Nuclear Power Plant

Internal exposures: Presentation of K. Mück, IRPA 10

External exposures (R. Meckbach, V. Chumak 1996):

Available data:

Gamma dose-rate measurements at 84 settlements in period 26 April (1 May)-31 May.

Individual occupancy histories for 19000 residents (type of residence, day of evacuation, for every day: settlement and time spent outdoors)

Procedure:

Plausibility checks of data

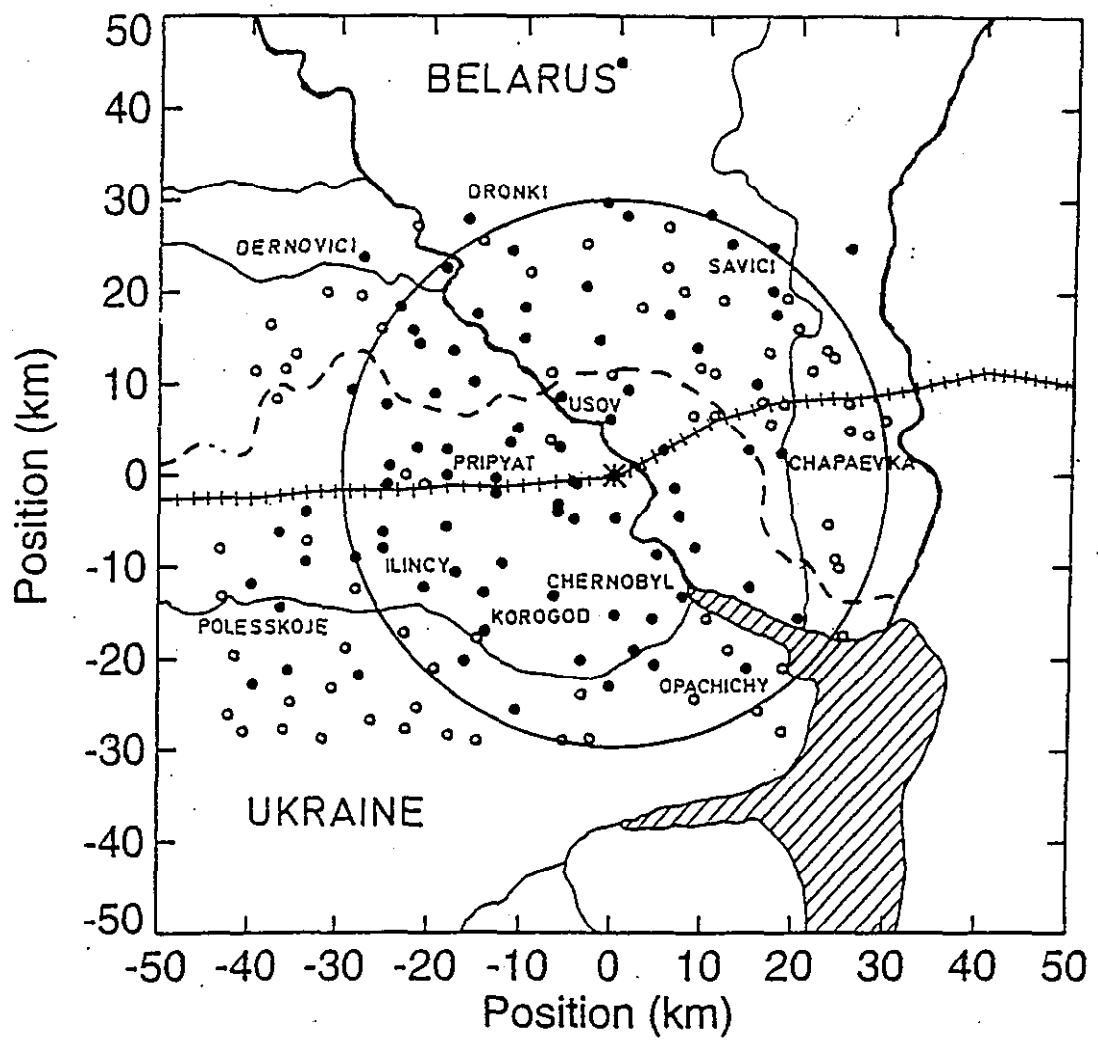
Interpolation in space (Kriging)

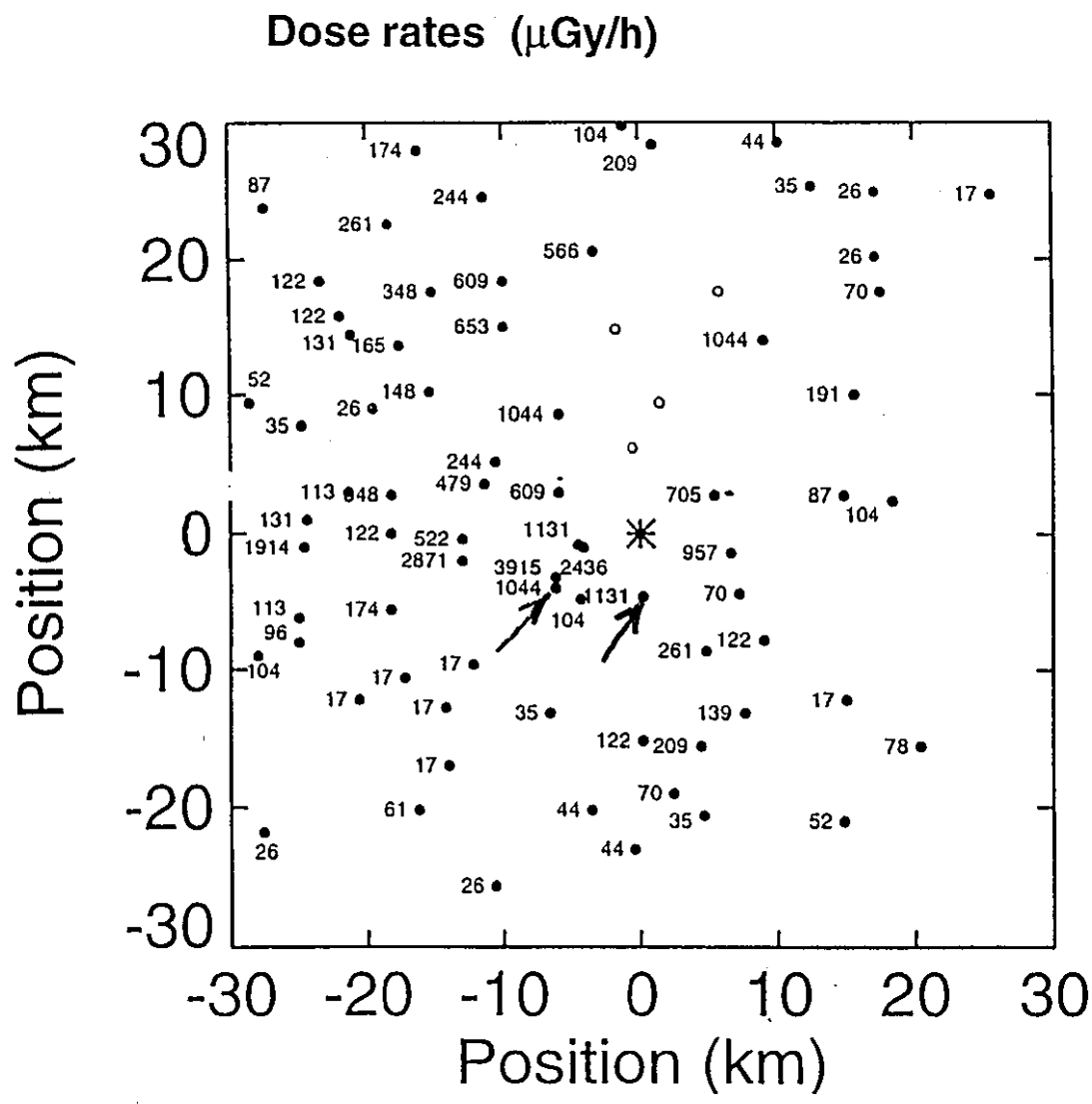
Extra- and interpolation in time

Evaluation of both interpolation schemes to derive gamma-dose rate over free fields

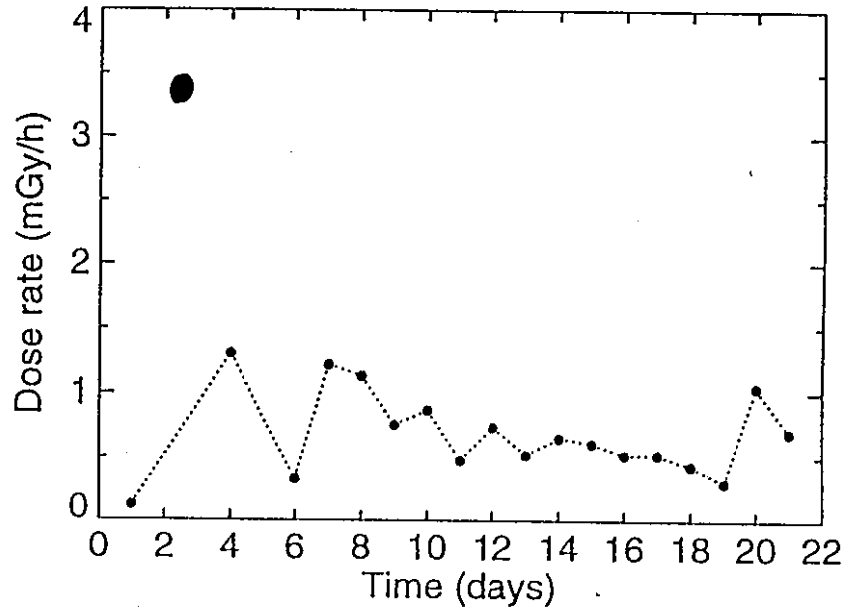
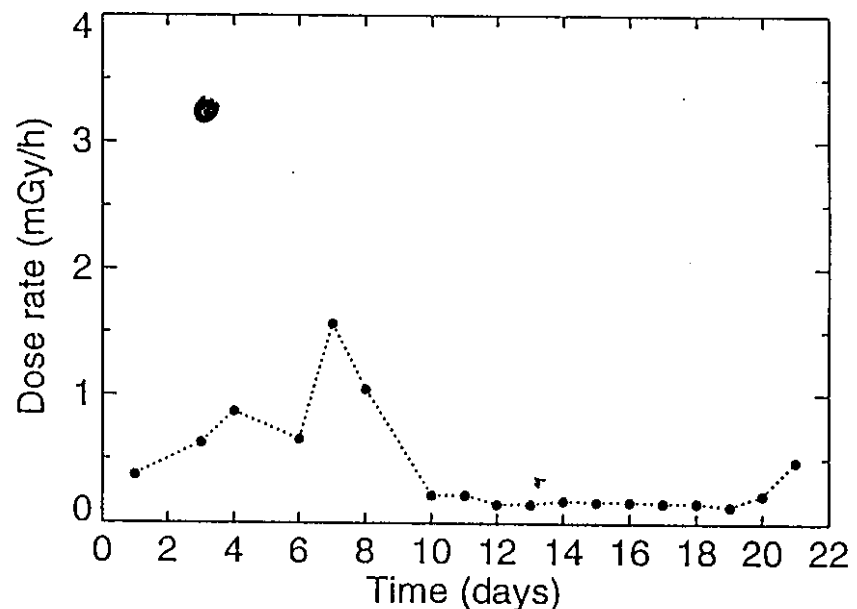
Application of location factors and occupancy times

Exclusion of evacuees having spent time in settlements for which gamma-dose rates could not be reconstructed reliably (remaining: 14 000 evacuees)





May 3 8th day



Kriging interpolations

The **interpolation weights** are determined from information on the **correlation** of the measured values in dependence of the **distance** between the measurement points

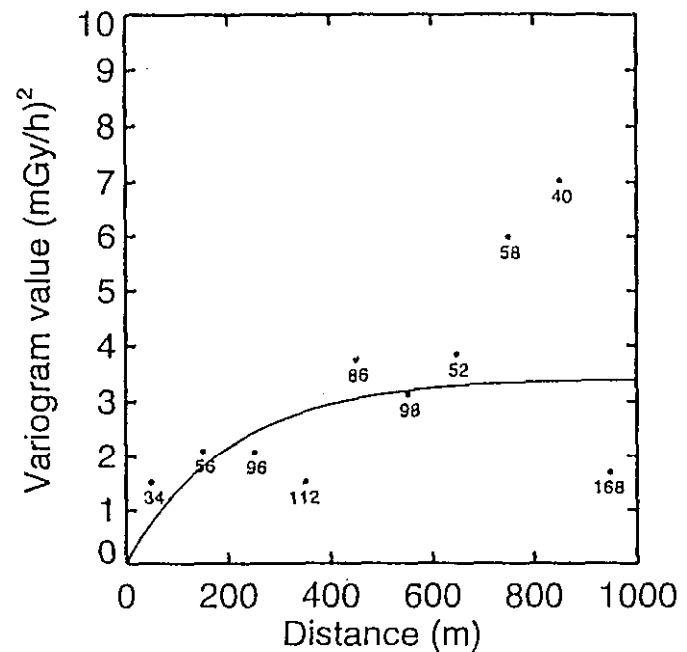
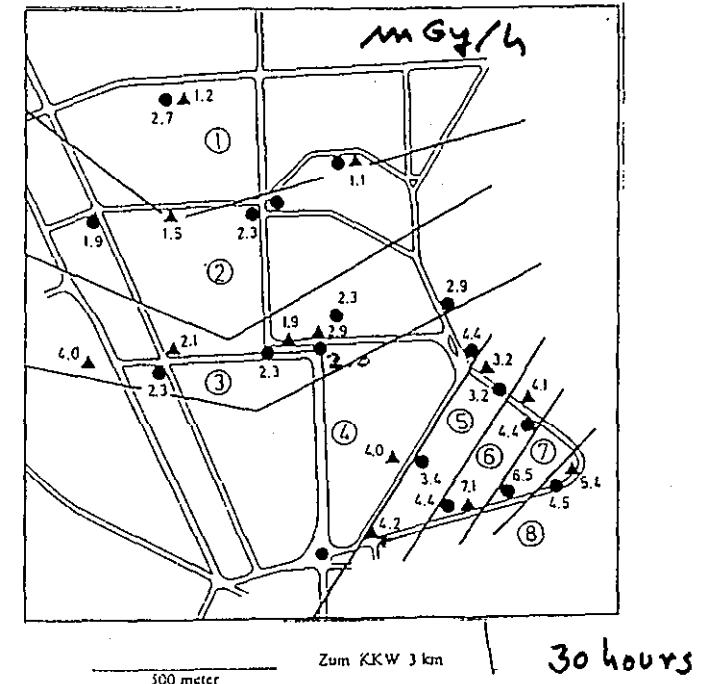
Variogram

$$V(h_k) = \frac{1}{2N(h_k)} \sum_{i,j} (D(\vec{x}_i) - D(\vec{x}_j))^2$$

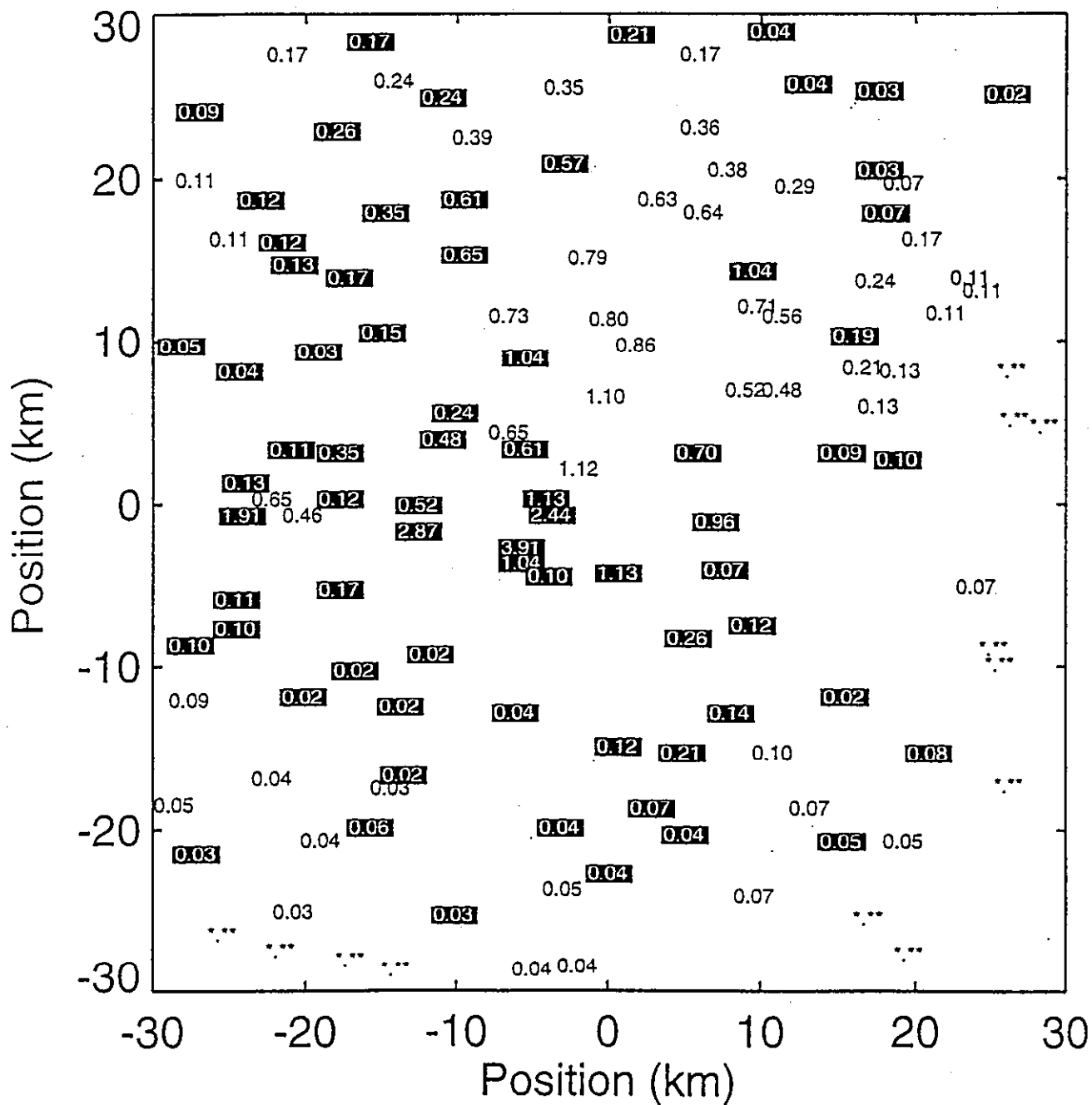
$$|\vec{x}_i - \vec{x}_j| \in h_k$$

Advantages:

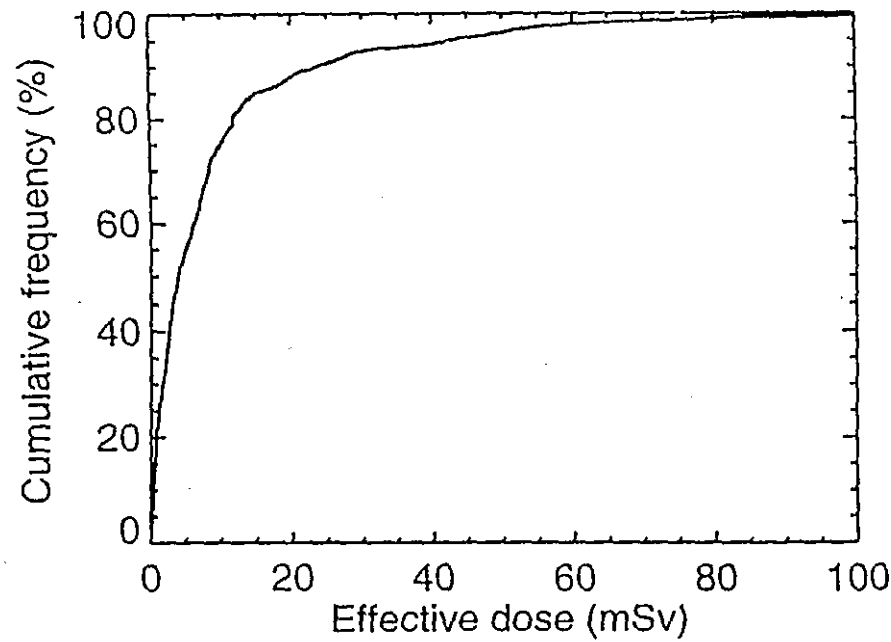
- declustering
- screening
- can account for anisotropy
- can allow for estimation of interpolation error



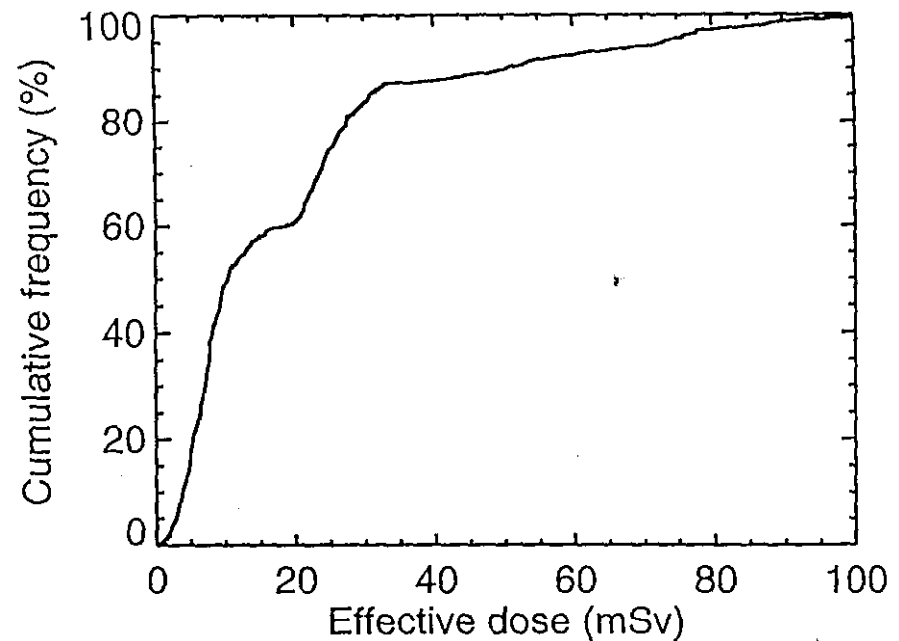
Kriging interpolations of dose rates (mGy/h)



May 3 8th day

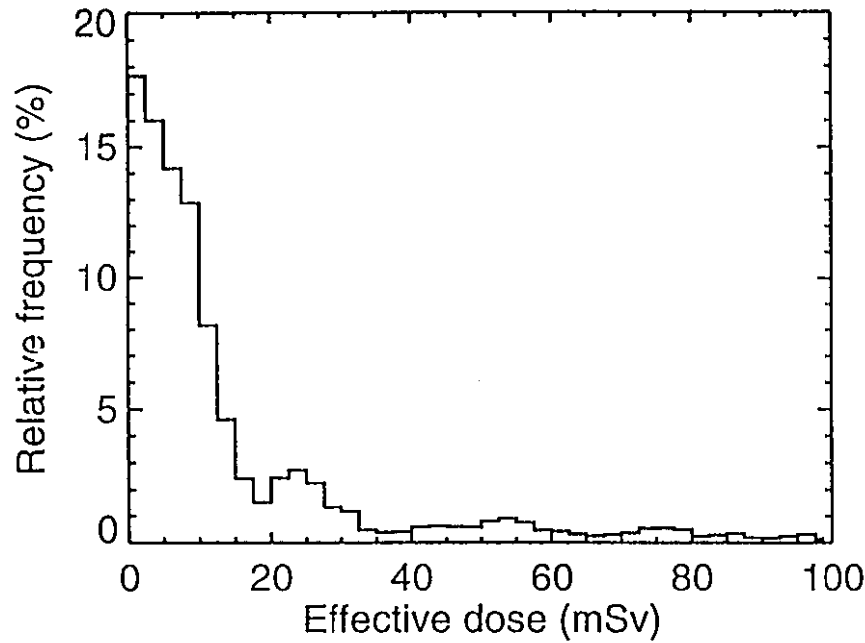


Cumulative distribution of individual external doses for 1628 schoolchildren from settlements of the 30 km zone.
Median: 3.8 mSv 95 percentile: 43 mSv



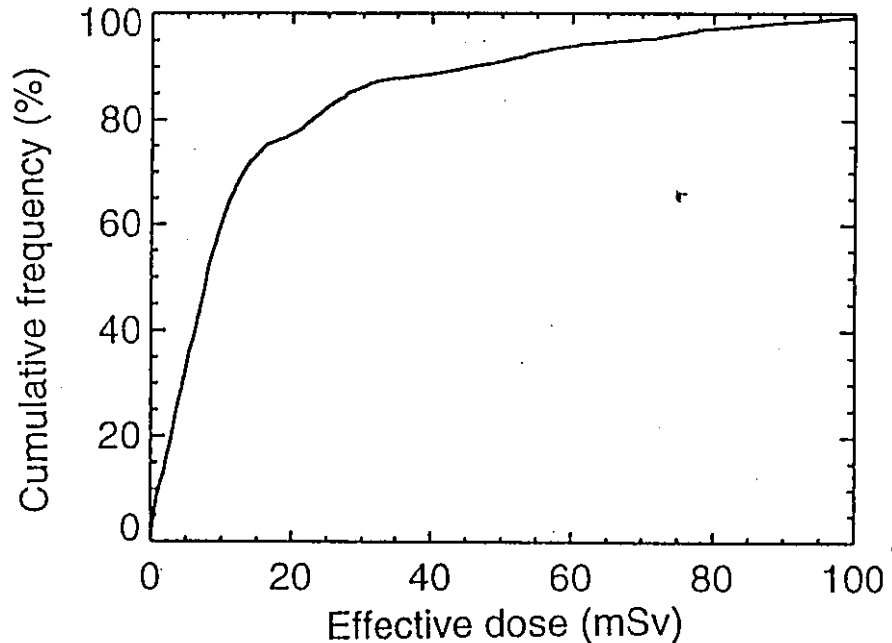
Cumulative distribution of individual external doses for 1915 agriculture workers from settlements of the 30 km zone.
Median: 10 mSv 95 percentile: 73 mSv

For 14084 evacuated persons from 30 km zone



**Distribution of
individual external doses**

arithmetic mean: 16 mSv
median: 7.8 mSv 95 percentile: 68 mSv
120 persons more than 100 mSv
maximum dose: 214 mSv



**Cumulative distribution of
individual external doses**

Dose Reconstruction for Workers of the Mayak Production Association

Jacob et al. (2000) Dose Reconstruction. GSF-Report 03/00

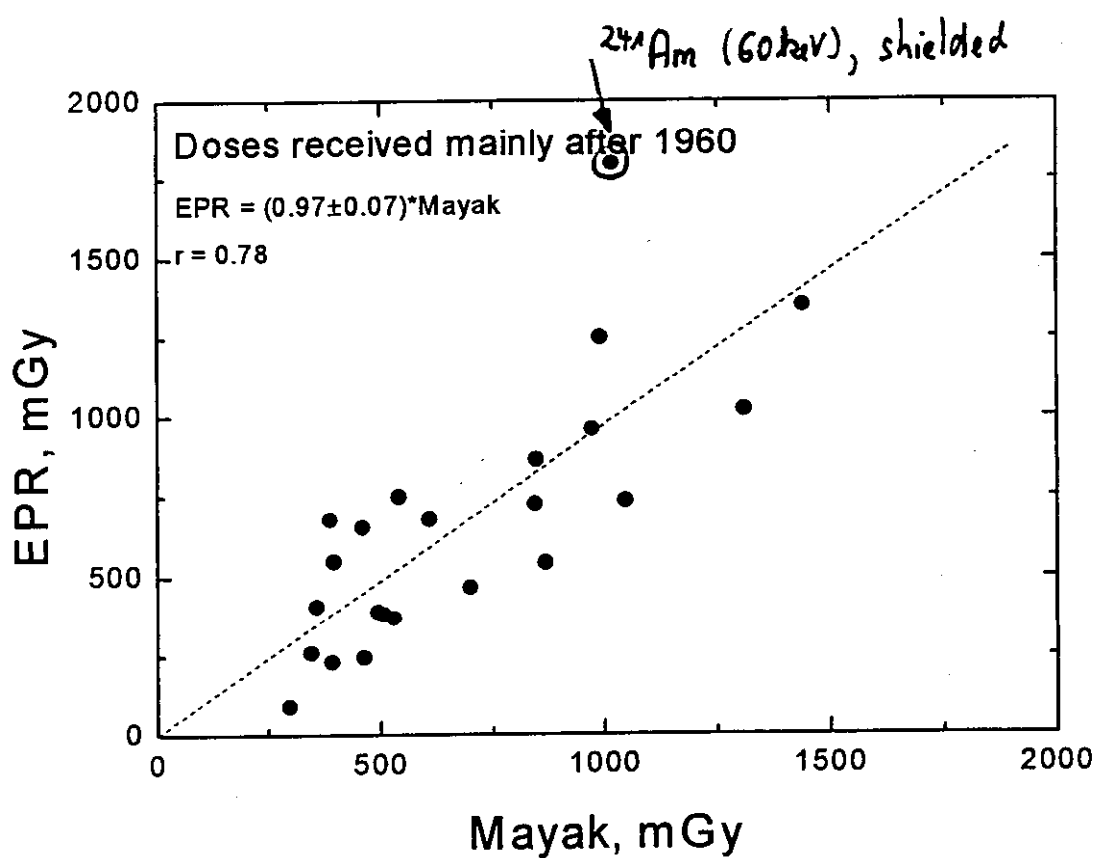
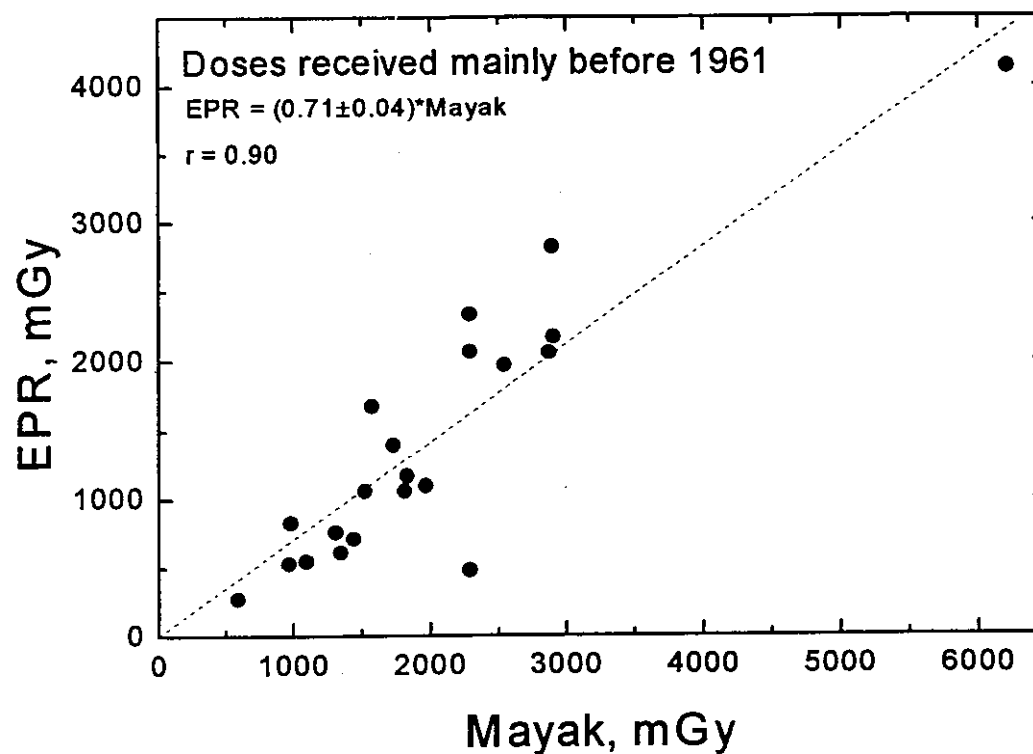
Cohort of 18 000 workers exposed in period 1948-1990

Occupational dosimetry before 1952 with films with high sensitivity in photon energy range of 20-100 keV, after 1961 with films with low sensitivity to photon energies below 50 keV.

Comparative analysis of occupational dosimetry with EPR (teeth) and FISH (chromosome aberrations) for about 100 workers.

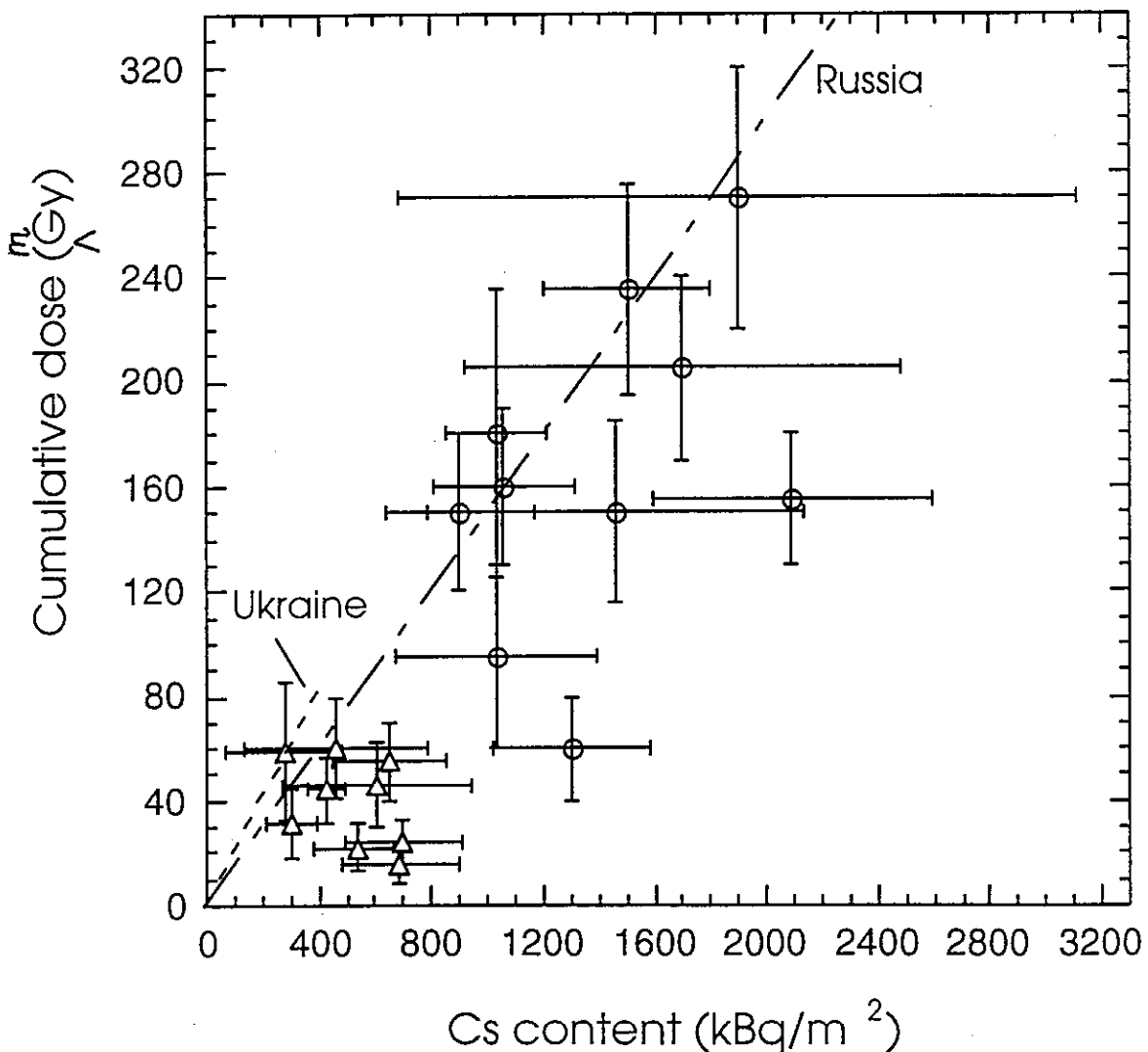
Good correlation between occupational dosimetry and EPR suggesting an overestimation of dose in the period before 1952 by occupational dosimetry.

Chromosome aberrations considerably lower than expected according to occupational dosimetry, large variability of ratio of dose estimates of the two methods.



Comparison of absorbed dose in air in populated areas (reconstructed from thermoluminescence measurements with bricks) and absorbed in air over an open field according to model calculations.

(After Bailiff et al. (2000). IN: Dose Reconstruction, GSF Report 03/00)



The average ^{137}Cs activity in soil (kBq m^{-2}) in the vicinity of the sample location vs the corresponding value of the cumulative dose $_{25\text{m}}\text{D}_x$, shown for all locations in Stary Vishkov and the Narodichy area. The dotted lines represent the cumulative dose predicted by the respective Russian and Ukraine models above undisturbed ground ($_{\text{RL}}\text{D}_{\text{cal}}$) calculated using the relevant DpA coefficients ($0.22 \text{ mGy}/(\text{kBq m}^{-2})$, Ukraine and $0.14 \text{ mGy}/(\text{kBq m}^{-2})$, Russia).

Conclusions

EPR Dosimetry:

Individual external radiation exposures.

Independent of time of exposure.

Detection limit $\leq 100 \text{ mSv}$.

Perspectives: Dependence on energy- and angular characteristics of radiation field, organ doses, in situ spectrometry.

Luminescence methods:

External radiation exposures of population groups.

Detection limit depending on time since production of ceramic material: $\geq 10 \text{ mSv}$.

Perspectives: Individual dosimetry, e.g. ceramic inlays.

Modelling:

Appropriate for larger population groups.

Particular useful in combination with instrumental methods.